

# Impact-induced melting and fragmentation of C-type asteroid regolith inferred from impact craters on a large Ryugu sample

C. Hamann<sup>1</sup>, E. Bonato<sup>2</sup>, A. Maturilli<sup>2</sup>, K. Mahlow<sup>1</sup>, M. Patzschke<sup>3</sup>, R. Luther<sup>1</sup>, K. Kurosawa<sup>4</sup>, G. Alemanno<sup>2</sup>, S. Schwinger<sup>2</sup>, A. Van den Neucker<sup>2</sup>, M. Baqué<sup>2</sup>, L. Hecht<sup>1,5</sup>, A. Greshake<sup>1</sup>, and J. Helbert<sup>2</sup>

<sup>1</sup>Museum für Naturkunde Berlin, 10115 Berlin, Germany. <sup>2</sup>German Aerospace Centre, 12489 Berlin, Germany. <sup>3</sup>Bruker Nano Analytics, 12489 Berlin, Germany. <sup>4</sup>Planetary Exploration Research Center, Chiba Institute of Technology, Narashino 275-0016, Japan. <sup>5</sup>Institute of Geological Sciences, Freie Universität Berlin, 12249 Berlin, Germany.

The surfaces of airless planetary bodies are continually exposed to hypervelocity impacts of micrometeoroids and the influx of solar-wind ions as well as electromagnetic radiation emitted from the sun or other galactic sources [1,2]. Over time, these processes gradually alter the morphologies, microstructures, and chemical compositions of regolith grains exposed to space [3–7], which is collectively known as space weathering. Because space weathering alters the optical properties of space-exposed regolith (e.g., [2]), understanding space weathering of various types of planetary surfaces is critical for interpretation of remote-sensing data obtained from such surfaces and for matching various meteorite types to potential parent bodies. However, while the effects of space weathering on anhydrous regolith materials is well understood on the basis of samples returned from the Moon (e.g., [3,4]) and S-type asteroid Itokawa (e.g., [5–7]), space weathering of hydrous, carbonaceous-chondrite (C-type) like asteroidal surfaces is poorly understood so far. Samples returned by JAXA’s Hayabusa2 mission from C-type near-Earth asteroid Ryugu (e.g., [8,9]) allow us to directly study the processes and products of space weathering of C-type asteroid regolith. Previous studies demonstrated that the uppermost surfaces of regolith grains returned from Ryugu’s surface are amorphous and dehydrated due to influx of solar-wind ions [10,11]. In addition, small microcraters typically less than 10 µm across and splashes of quenched melt—presumably impact melts—have been reported from several Ryugu samples [10,12]. To better understand the role of micrometeoroid impacts in space weathering of C-type asteroids, we studied the impact-crater population on Ryugu sample A0112, which is a large (3.0 × 1.8 mm) regolith grain collected at the first touchdown site from the asteroid’s immediate surface.

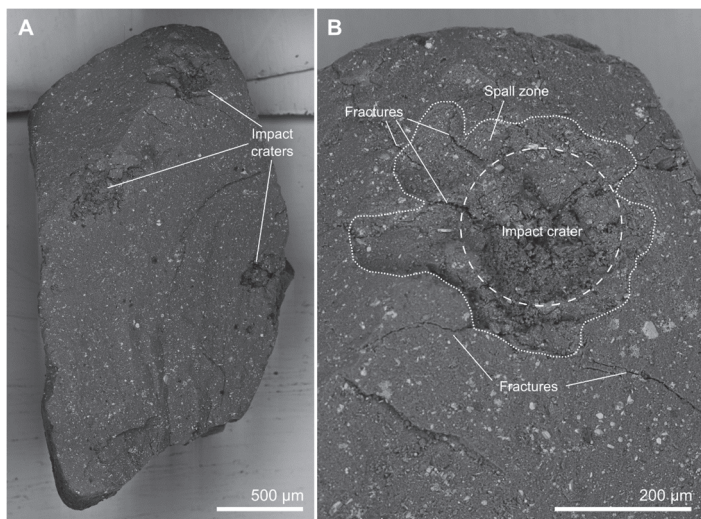


Figure 1. SEM-BSE images of the crater-covered side of A0112 (A) and the largest impact crater surrounded by a spall zone and surface-related, impact-produced fractures (B).

Scanning electron microscopy (SEM) at Museum für Naturkunde Berlin, Germany and Bruker Nano Analytics, Berlin, Germany as well as X-ray micro-computed tomography ( $\mu$ CT) at Museum für Naturkunde Berlin revealed the presence of three large, crater-like depressions of 150–270 µm diameter as well as of several smaller, circular pits of between 5 and 20 µm diameter on one of the surfaces of A0112 (Fig. 1). High-magnification SEM imaging furthermore revealed the presence of frothy, highly vesicular materials that are interpreted as quenched impact melts (cf. [10]) lining the bottoms and walls of the large and many of the small crater-like depressions (Fig. 2). Reflectance spectra obtained at German Aerospace Centre, Berlin, Germany from the frothy material lining the largest crater-like depression are almost featureless between 2 and 4 µm (Fig. 3) and resemble those obtained from the CI chondrite Ivuna heated to 700 °C [13]. Control

spectra obtained from the non-crater-bearing sides of A0112 are consistent with infrared spectra of other Ryugu samples (e.g., [14]) and showed pronounced spectral features at 2.71 µm and 3.32 and 3.46 µm that correspond to OH-bearing phyllosilicates and carbonates, respectively. Elemental analysis by energy dispersive X-ray spectroscopy (EDS) and EDS element distribution maps showed that the frothy materials are quenched silicate–sulfide emulsions, which suggests that the crater-like depressions and pits are impact craters. Quenched melt splashes up to 300 µm across exist not only on the crater-bearing side of A0112, but also on an additional side of the sample. These are similar in chemical composition to the frothy layers described recently from other Ryugu samples [10] and invariably comprise silicate–sulfide emulsions. High-resolution EDS element distribution maps furthermore suggest that the quenched melts contain immiscible FeNi metal droplets (cf. [11]). In terms of major-element

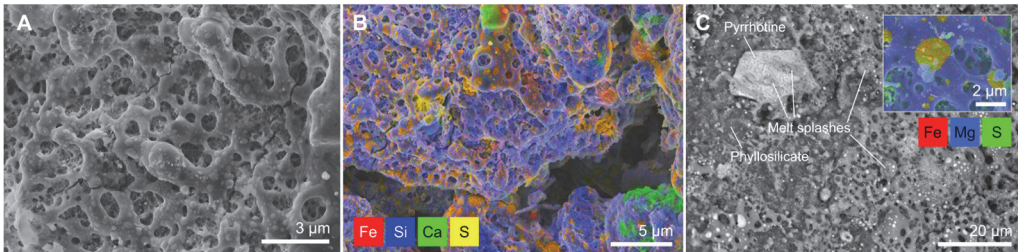


Figure 2. SEM-SE image (A) and element distribution map (B) of quenched impact melts lining the bottoms of the large impact craters on A0112. (C) SEM-BSE image of quenched melt splashes on the surface of A0112. A high-magnification element distribution map of the quenched melt splashes is shown in the inset.

subsurfaces adjacent to and below the large craters are intensely fractured; in particular, we observed fracture patterns resembling radial, concentric, and spallation fractures known from impact experiments in the strength regime (e.g., [17] and references therein). Consistent with lunar microcraters [17], large craters  $>150 \mu\text{m}$  are surrounded by irregular spallation zones whereas small craters  $<40 \mu\text{m}$  are almost perfectly bowl-shaped.

While investigations on the impact craters and quenched melts on A0112 are ongoing, our preliminary results provide information on the nature and magnitude of impact-induced processing of C-type asteroid surfaces in relation to solar wind-induced space weathering. Sample A0112 appears to be the most intensely shocked Ryugu sample investigated so far—the majority of smaller Ryugu samples were so far reported to be either essentially unshocked [18] or only marginally affected by micrometeoroid impacts, with solar wind-derived modifications dominating over impact-induced modifications [10–12]. Our findings of relatively large craters and abundant quenched impact melts on A0112 suggests that micrometeoroid impacts play an equally important role in space weathering of C-type asteroid regoliths as solar-wind induced modifications do. Impact-induced fracturing and spallation associated with the large craters on A0112 also informs on the efficiency of impact-induced fragmentation of grains in C-type asteroid regoliths [19]: Our observations suggest that spallation zones of micrometeoroid impact craters are likely sources of hydrated carbonaceous micrometeoroids arriving on Earth, contradictory to recent proposals based on unshocked to mildly shocked Ryugu grains [18]. This hypothesis is based on the fact that spall fragments ejected from spall zones surrounding hypervelocity impact craters are typically unshocked (e.g., [20]), but detailed numerical models using the iSALE shock physics code are currently being computed to probe peak pressures and temperatures in the spall zones surrounding the craters on A0112. If A0112’s microcrater population is representative of Ryugu’s surface, our results have relevance for evaluation of the relative roles of thermal [21,22] vs. impact-triggered [17] comminution of, and dust production from, C-type asteroid regolith.

Acknowledgments: We thank JAXA for allocation of Ryugu sample A0112.

chemistry, the melt splashes on A0112 match fusion crusts around the CI chondrites Orgueil and Alais [15] and resemble a quenched melt particle of likely impact-melt origin recently reported from Orgueil [16]. Furthermore, µCT scans revealed that the

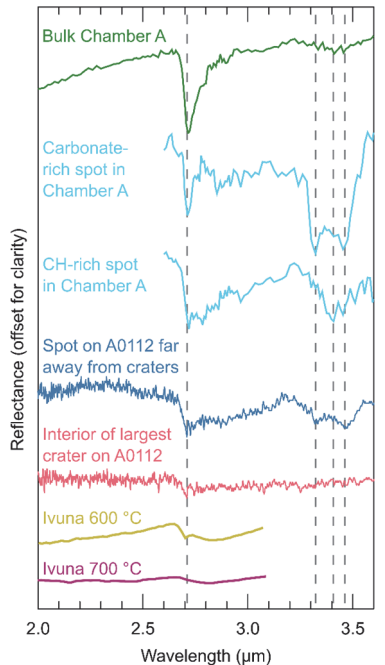


Figure 3. Reflectance spectra obtained from the largest impact crater on A0112 (red) compared against a spot far away from the craters (blue). Also shown are spectra of bulk A particles (green; [14]), carbonate- and CH-rich spots on Chamber A particles (light blue; [14]), and heated Ivuna CI chondrite (yellow and pink; [13]) for comparison.

## References

- [1] Hapke B. 2001. *Journal of Geophysical Research Planets* 106: 10039–10073.
- [2] Pieters C. M. and Noble S. K. 2016. *Journal of Geophysical Research Planets* 121: 1865–1884.
- [3] Keller L. P. and McKay D. S. 1997. *Geochimica et Cosmochimica Acta* 64: 2331–2341.
- [4] Pieters C. M. et al. 2000. *Meteoritics & Planetary Science* 35: 1101–1107.
- [5] Noguchi T. et al. 2011. *Science* 333: 1121–1125.
- [6] Noguchi T. et al. 2014. *Meteoritics & Planetary Science* 49: 188–218.
- [7] Thompson M. S. et al. 2014. *Earth, Planets and Space* 66: 89.
- [8] Yokoyama T. et al. 2023. *Science* 379: eabn7850.
- [9] Nakamura T. et al. 2023. *Science* 379: eabn8671.
- [10] Noguchi T. et al. 2023. *Nature Astronomy* 7: 170–181.
- [11] Melendez L. E. et al. 2023. Abstract #6286. 86<sup>th</sup> Meteoritical Society Meeting.
- [12] Nakato A. et al. 2023. *Earth, Planets and Space* 75: 45.
- [13] Hiroi T. and Pieters C. M. 1996. Abstract #551. 27<sup>th</sup> LPSC.
- [14] Pilorget C. et al. 2022. *Nature Astronomy* 6: 221–225.
- [15] Genge M. H. and Grady, M. M. 1999. *Meteoritics & Planetary Science* 34: 341–356.
- [16] Zolensky M. et al. 2022. *Meteoritics & Planetary Science* 57: 1902–1919.
- [17] Hörz F. et al. 2020. *Planetary and Space Science* 194: 105105.
- [18] Tomioka N. et al. 2023. *Nature Astronomy* 7: 669–677.
- [19] Flynn, G. J. 2009. *Planetary and Space Science* 57: 119–126.
- [20] Melosh H. J. 1984. *Icarus* 59: 234–260.
- [21] Delbo M. et al. 2014. *Nature* 508: 233–236.
- [22] Delbo M. et al. 2022. *Nature Geoscience* 15: 453–457.